Variational Entanglement-Assisted Quantum Process Tomography with Arbitrary Ancillary Qubits

Shichuan Xue,[1,†] Yizhi Wang,[1,†] Junwei Zhan,[1] Yaxuan Wang,[1] Ru Zeng,[1] Jiangfang Ding,[1] Weixu Shi,[1] Yong Liu,[1] Yingwen Liu,[1] Anqi Huang,[1] Guangyao Huang,[1] Chunlin Yu,[2] Dongyang Wang,[1] Xiang Fu,[1] Xiaogang Qiang,[3] Ping Xu,[1] Mingtang Deng,[1] Xuejun Yang,[1] and Junjie Wu[1,*]

[1]*Institute for Quantum Information & State Key Laboratory of High Performance Computing, College of Computer Science and Technology, National University of Defense Technology, Changsha 410073, China*

[2]*China Greatwall Research Institute, China Greatwall Technology Group CO., LTD., Shenzhen 518057, China*

[3]*National Innovation Institute of Defense Technology, AMS, Beijing 100071, China*

(Received 29 May 2022; revised 8 September 2022; accepted 8 September 2022; published 23 September 2022)

Quantum process tomography is a pivotal technique in fully characterizing quantum dynamics. However, exponential scaling of the Hilbert space with the increasing system size extremely restrains its experimental implementations. Here, we put forward a more efficient, flexible, and error-mitigated method: variational entanglement-assisted quantum process tomography with arbitrary ancillary qubits. Numerically, we simulate up to eight-qubit quantum processes and show that this tomography with m ancillary qubits ($0 \leq m \leq n$) alleviates the exponential costs on state preparation (from 4^n to 2^{n-m}), measurement settings (at least a 1 order of magnitude reduction), and data postprocessing (efficient and robust parameter optimization). Experimentally, we first demonstrate our method on a silicon photonic chip by rebuilding randomly generated one-qubit and two-qubit unitary quantum processes. Further using the error mitigation method, two-qubit quantum processes can be rebuilt with average gate fidelity enhanced from 92.38% to 95.56%. Our Letter provides an efficient and practical approach to process tomography on the noisy quantum computing platforms.

DOI: 10.1103/PhysRevLett.129.133601

Introduction.—With the rapid development of quantum computing devices in recent years, the quantum computing systems scale to over fifty available qubits [1–3]. Hence, efficient and practical quantum certification and benchmarking appear to be increasingly essential in the noisy intermediate-scale quantum (NISQ) era [4–7]. Various protocols have been proposed, including direct fidelity estimation [8], randomized benchmarking [9,10], and so on; nevertheless, quantum process tomography (QPT) still plays an indispensable role, since it is a comprehensive characterization of quantum systems with full information.

However, standard QPT [11,12] is an inefficient and resource-demanding procedure. Specifically, standard QPT needs 4^n input states and consequent quantum state tomography (QST) for each state, and the total number of quantum measurements scales as 4^{2n} for an n-qubit quantum process [13]. Besides, solving the inverse problem of state estimation involves huge computational costs [14,15]. Such exponential expenditures on space, time, and computation are tremendous for practical usages; hence, it is physically feasible only up to three-qubit case from the point of experiment [16–22]. Many proposals are put forward to address these problems, including compressed sensing tomography [19,23] and ansatz-based tomography [24], but at the cost of stronger assumptions (e.g., sparsity requirements, low-rank or specific tensor-product structure) and hence not applicable to general conditions. Entanglement-assisted process tomography (EAPT) [25–27] uses the intrinsic relation between QST and QPT based on Choi-Jamiolkowski isomorphism [28,29] and imprints complete information about a quantum process on its output state [30]. However, there still needs to be a complete QST procedure on the output states in the extended Hilbert space. And it introduces an ancillary space as great as the system space and consumes double amounts of qubits. Thus, the experimental realization is realized on bulk optical platforms up to one-qubit cases [25,31].

In this Letter, we put forward a more efficient, flexible, and error-mitigated method: variational entanglement-assisted process tomography (VEAPT) with arbitrary ancillary qubits. The overall scheme is illustrated in Fig. 1(a).

To enhance the efficiency, we first introduced the variational quantum algorithm (VQA) [33–41] to alleviate

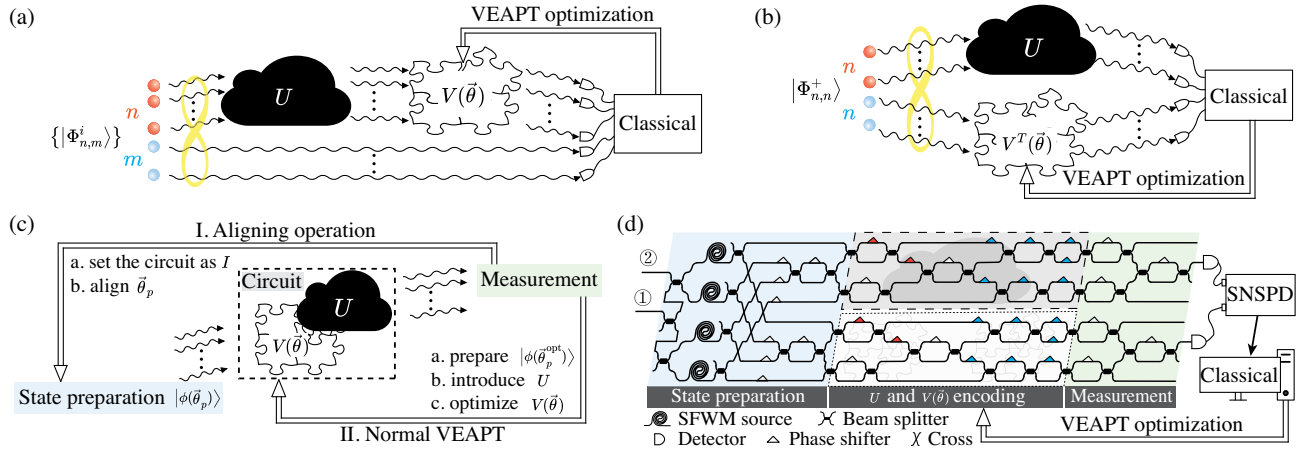

FIG. 1. (a) Structure of the VEAPT with arbitrary ancillary qubits. The scheme consists of the preparation of input entanglement states, the evolution of the unknown channel and the controllable process, and the classical processing unit. The classical part is composed of cost function evaluation, classical optimization, and parameter updating. (b) Structure of the VEAPT with full ancillaries. It is a specialized version of VEAPT in that the $V(\vec{\theta})$ process can be transposed to the ancillary space by quantum ricochet property when the ancillary qubits are full. (c) Scheme of the error mitigation method. The first stage is the aligning operation by directly setting the circuit as I. The second stage is the normal VEAPT optimizing with target U and encoding $V(\vec{\theta})$. (d) Photonic chip structure and experimental realization. When the ancillary qubits are arbitrary, the laser is inputted at the first layer of the beam splitter network (denoted as ①). When the ancillaries are full, it pumps in the second layer (denoted as ②). In the encoding circuit part, we give an illustration of the VEAPT with full ancillaries [the dashed box denotes U and the dotted box denotes $V^T(\vec{\theta})$]. The red colored phase shifters are for one-qubit process encoding, while the blue colored ones are for the two-qubit case. More details are provided in the Supplemental Material [32].

the data postprocessing. Specifically, we transformed the complicated QST procedure into a more efficient optimization problem of the parametrized circuit. Second, we combined the EAPT approach to fully exploit the quantum parallelism of entanglement and reduce the input states' preparations.

In terms of the flexibility, we put forward the VEAPT theory with arbitrary ancillary qubits. We proved that for an n-qubit arbitrary unitary process, VEAPT with m ancillary qubits ($0 \le m \le n$) needs 2^{n-m} entangled states as inputs to rebuild the quantum process.

The VEAPT method shows the inherent tolerance to state preparation and measurement error and shot noise. Besides, we further put forward an error mitigation method [42,43] based on the simplified VEAPT structure with fixed and flexible input states and efficient measurements.

Numerically, we conducted simulations based on the variational quantum circuit simulator to eight-qubit quantum processes and results present the alleviation of the exponential costs on state preparation (from 4^n to 2^{n-m}), measurement settings (at least 1 order of magnitude fewer measurements), and data postprocessing.

Experimentally, we designed a silicon photonic chip shown in Fig. 1(d) and demonstrated our method on one-qubit and two-qubit randomly generated unitary quantum processes. Results show good consistency with our theory and present robustness in terms of shot noises and enhanced performance with error mitigation method.

Efficient VEAPT with full ancillary qubits.—For an n-qubit quantum process, the standard EAPT needs to introduce n ancillary qubits and construct one $2n$-qubit maximally entangled state $|\Phi^+_{n,n}\rangle = (1/\sqrt{d})\sum_{j=1}^{d}|j\rangle \otimes |j\rangle$ as input, where $d = 2^n$. Then, based on Choi's proof in Ref. [28,29], we can obtain the Kraus operator-sum representation of the process $\mathcal{E}(\rho) = \sum_k (A_k \otimes I_{\mathrm{anc}})\times \rho(A_k \otimes I_{\mathrm{anc}})^\dagger$ once we have done the full QST on the output $\mathcal{E}(\rho)$, where $\rho = |\Phi^+_{n,n}\rangle\langle\Phi^+_{n,n}|$, A_k are the Kraus operators, and I_{anc} denotes no operation on the ancillary space.

Furthermore, we introduced the VQA framework [44,45] to the EAPT procedure following the two steps to further enhance the performance of the data postprocessing.

First, we fixed the quantum process output state identical to the input, therefore avoiding the QST procedure on the output. It can be deduced from Choi's conclusion that when the output is the same as the input, the overall quantum process is $I_{\mathrm{sys}} \otimes I_{\mathrm{anc}}$. It is also feasible to set the output state as a known and fixed state $(R_{\mathrm{sys}} \otimes I_{\mathrm{anc}})|\Phi^+_{n,n}\rangle$. Here, for simplicity, we chose the identical input and output states. Second, we transformed the data postprocessing structure into a variational framework. Specifically, we introduced a parametrized controllable process $V(\vec{\theta})$ as the variational target, which follows the unknown process U. The variational process is to update the parameter list $\vec{\theta}$ and minimize the infidelity between the output state and the input state based on the direct fidelity estimation method. It

is worth noting that under the maximally entangled states $|\Phi^+_{n,n}\rangle$, we could transpose the $V(\vec{\theta})$ circuit to the ancillary space based on the quantum ricochet property as shown in Fig. 1(b). Hence, the cost function is defined as

$$f(\vec{\theta}) = 1 - F(|\Phi^+_{n,n}\rangle, (V(\vec{\theta})U \otimes I)|\Phi^+_{n,n}\rangle) = 1 - F(|\Phi^+_{n,n}\rangle, [U \otimes V^T(\vec{\theta})]|\Phi^+_{n,n}\rangle), \quad (1)$$

where F denotes the fidelity measure. When the cost function $f(\vec{\theta})$ goes down to zero, we can arrive at $V(\vec{\theta})U = I$. Therefore, the controllable parameters in the $V(\vec{\theta})$ can be directly used to rebuild the quantum process U without complicated data postprocessing.

In the variational optimizing procedure, our framework accepts all efficient algorithms flexibly. In this Letter, we take the typical iterative method for solving unconstrained nonlinear problems—Broyden-Fletcher-Goldfarb-Shanno (BFGS) algorithm [46–49]—and the gradient-based simultaneous perturbation stochastic approximation (SPSA) [50] algorithm as examples. We numerically and experimentally verified these two algorithms (more details provided in the Supplemental Material [32]).

Flexible VEAPT with arbitrary ancillary qubits.—The VEAPT method alleviates the state preparation and data postprocessing burdens. However, it constrains the input as a faithful state ρ by requiring the Schmidt number $\mathrm{Sch}(\rho) = d^2$, thus demanding the ancillary space as great as the system space [30]. Hence, it suffers from at least double amounts of qubits, which is quite an overhead and waste for quantum devices since the ancillary qubits undergo no operations at all in the protocol. Therefore, we take the more general and flexible ancillary conditions into consideration as shown in Fig. 1(a). We proved that for an n-qubit arbitrary unitary process, VEAPT with m ancillary qubits $(0 \le m \le n)$ needs to prepare 2^{n-m} entangled states as inputs to rebuild the quantum process. Below we give theoretical explanations.

The VEAPT method fully exploits the most important advantage of quantum computing: quantum parallelism. By preparing a maximally entangled state $|\Phi^+_{n,n}\rangle$, the information of the system is completely imprinted in the quantum entanglement. Actually, tracing out the ancillary space, the remaining system state is in a superposition of all computational basis $\mathrm{Tr}_{\mathrm{anc}}(|\Phi^+_{n,n}\rangle\langle\Phi^+_{n,n}|) = (1/2^n)\sum_{i=1}^{2^n}|i\rangle\langle i|$. Hence, such a maximally entangled state can simultaneously calculate the dynamics for all the basis.

Similarly, when the ancillary qubits m is less than the system qubits n, there still exists partial maximally entanglement between the m ancillary and m system qubits, which contain 2^m basis components in an output state. Under such case, it is natural to divide the total 2^n basis into $2^n/2^m = 2^{n-m}$ states. Each state couples the 2^m entangled terms $|i\rangle_{\mathrm{sys}}|i\rangle_{\mathrm{anc}}$ with one of the remaining 2^{n-m} basis $|j\rangle_{\mathrm{sys}}$ to construct the superposition. Hence, the 2^{n-m} states are

$$|\Phi^j_{n,m}\rangle = \frac{1}{\sqrt{2^m}}\sum_{i=1}^{2^m}(|i\rangle_{\mathrm{sys}} \otimes |i\rangle_{\mathrm{anc}}) \otimes |j\rangle_{\mathrm{sys}}, \quad j = 1 \ldots 2^{n-m}. \quad (2)$$

It can be seen that when $m = n$, the needed one input is the $|\Phi^+_{n,n}\rangle$ in EAPT.

Combined with the variational framework, we can give the following theoretical analysis. For VEAPT with m ancillaries, the quantum process is extended to $U_{2^n,2^n} \otimes I_{2^m,2^m}$, and based on the above 2^{n-m} input states, we have that for $j = 1 \ldots 2^{n-m}$,

$$\sum_{i=1}^{2^m} U|i\rangle_{\mathrm{sys}}|j\rangle_{\mathrm{sys}} \otimes I|i\rangle_{\mathrm{anc}} = \sum_{i=1}^{2^m}|i\rangle_{\mathrm{sys}}|j\rangle_{\mathrm{sys}} \otimes |i\rangle_{\mathrm{anc}}. \quad (3)$$

By multiplying arbitrary basis $\langle xyz|$ to Eq. (3), we obtain

$$\sum_{i=1}^{2^m}\langle xy|U|ij\rangle\langle z|i\rangle = \sum_{i=1}^{2^m}\langle x|i\rangle\langle y|j\rangle\langle z|i\rangle, \quad U_{xy,ij} = \delta_{ix}\delta_{jy}. \quad (4)$$

Hence, only diagonal elements in U are equal to 1. By keeping the 2^{n-m} outputs identical to the inputs, the quantum process is fixed at I.

So, VEAPT with m ancillaries lowers the demands for the ancillary qubits and offers a flexible and practical method to determine the input states considering the physical qubit resources. It is noted that the generality is maintained and still applicable to arbitrary unitary processes.

Besides, the VEAPT method has advantages to tackle the QPT problem in the NISQ background. On the one hand, it has an inherent robustness toward state preparation and measurement errors and shot noises since the lower demands on input states and the simplified data processing with variational framework help to decrease the error sources. Moreover, it has the capability to conduct the error mitigation method as shown in Fig. 1(c). There are two stages primarily. In the aligning operation stage, by setting the circuit as an identity process in advance, it can align the state preparation parameters $\vec{\theta}_p$ to eliminate the relative deviations under noisy conditions. Here, the cost function defines as the infidelity between the preparation state and the measurement basis. After the aligning, we obtain the optimal input state $|\phi(\vec{\theta}_p^{\mathrm{opt}})\rangle$. In the normal VEAPT stage, we prepare the input state at the aligned optimal state $|\phi(\vec{\theta}_p^{\mathrm{opt}})\rangle$, and conduct the consequent VEAPT optimizations with U and $V(\vec{\theta})$ introduced.

It is worth noting that the error mitigation feature is based on the generalized EAPT theory (fixed state

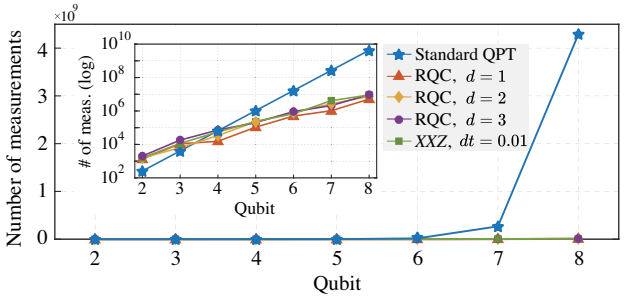

FIG. 2. Numerical simulations on variational quantum circuit simulator for RQC with different circuit depth d and Heisenberg XXZ spin chain time evolution quantum processes up to eight-qubit cases. It is obvious that the VEAPT method significantly decreases the total number of measurements compared to standard QPT (blue starred line) when the qubit number scales. Furthermore, in the inset graph, we present the graph in the logarithmic axis and obtain a clear and enlarged measurement gap (at least a 1 order of magnitude reduction).

preparation) and variational data postprocessing (simplified state measurement). Hence, these three features are inseparably interconnected and complement each other to fulfill collaborated efforts toward an efficient, flexible, and error-mitigated VEAPT method in the NISQ era.

Numerical and experimental demonstration.—We first conducted numerical simulations on two types of quantum processes up to eight-qubit cases—d-depth randomly generated quantum circuit (RQC) [51,52] and Heisenberg XXZ spin chain [53] with evolution time $dt = 0.01$—using the variational quantum circuit simulator. The total number of measurements is illustrated in Fig. 2. It is clear that the measurement settings are at least 1 order of magnitude fewer than the standard QPT and the gap tendency appears to be larger with the system size increasing. Details are provided in the Supplemental Material [32].

Experimentally, silicon photonic chips have made considerable progress in quantum computing, including entanglement generation [54], quantum control [55], and application [56]. Based on the VEAPT method, we designed a silicon photonic chip and conducted an experimental demonstration on it. The chip structure is illustrated in Fig. 1(d), which consists of three parts: entangled state generation, quantum process [unknown U and controllable $V(\vec{\theta})$] encoding, and measurement.

In terms of the entangled state generation, the chip contains a tree-organized beam splitter network and four spontaneous four-wave mixing photon-pair sources to prepare several simple and fixed input states. In the encoding part, we imprinted the quantum process information as the phase shifters' values $\vec{\theta}$. Figure 1(d) shows the VEAPT with full ancillaries configuration, where the dashed box denotes U and the dotted box denotes $V^T(\vec{\theta})$. Under such a condition, we used both system space and ancillary space to encode the information that increases the encoding degree and decreases the circuit depth. More details are provided in the Supplemental Material [32]. Finally, in the measurement part, we conducted the direct fidelity estimation to obtain the cost function values. In the classical processing part, the VQA takes cost function evaluation values, uses classical optimization methods to calculate its gradient, and updates the circuit parameters. As a whole, the VEAPT method is a quantum-classical hybrid architecture.

Here, we evaluate experimental results using the average gate fidelity [57]. The average gate fidelity F_{avg} between the rebuilt U and the real $\mathcal{E}$ is given by $F_{\text{avg}}(\mathcal{E}, U) = \int d\psi \langle\psi|U^\dagger \mathcal{E}(|\psi\rangle\langle\psi|)U|\psi\rangle$. For VEAPT with full ancillaries, we experimentally demonstrated one-qubit and two-qubit cases. Specifically, for one-qubit VEAPT, the input two-qubit entangled state is $|\Phi^+_{1,1}\rangle = (|00\rangle + |11\rangle)/\sqrt{2}$, while in the two-qubit VEAPT case, the four-qubit input entangled state is $|\Phi^+_{2,2}\rangle = (|0000\rangle + |0101\rangle + |1010\rangle + |1111\rangle)/2$. And in the encoding section, we randomly generated phase shifters to encode the unknown U information. Correspondingly in the decoding part, phase shifters are used to recover the values. The initial values of the optimization are set at the orthogonal position with the answer to present a complete optimization process from one to zero. Figure 3(a) gives the experimental results of VEAPT with full ancillaries, where the maximum average gate fidelities are 99.73% and 93.33%, respectively.

Moreover, we also verified the VEAPT with fewer ancillaries and conducted the experiment of two-qubit QPT with one ancillary qubit. Under such conditions, there needs to be two input entangled states: $|\Phi^1_{2,1}\rangle = (|000\rangle + |101\rangle)/\sqrt{2}$ and $|\Phi^2_{2,1}\rangle = (|010\rangle + |111\rangle)/\sqrt{2}$, as Eq. (3) shows. The cost function is the sum of the two infidelities $f(\vec{\theta}) = 2 - |\langle\Phi^1_{2,1}|\phi^{\text{out}}_1\rangle|^2 - |\langle\Phi^2_{2,1}|\phi^{\text{out}}_2\rangle|^2$, where $|\phi^{\text{out}}_i\rangle$ corresponds to the output state of $|\Phi^i_{2,1}\rangle$. It is clear in Fig. 3(b) that the two infidelities converge quickly, and the final quantum gate fidelity could reach over 97%.

Besides, we also demonstrated the capability of error mitigation and the robustness toward shot noises in the NISQ background. The VEAPT structure greatly simplifies the frontier state preparation and back-end measurement, thus, facilitating the error mitigation operations. Specifically in the aligning stage, the parameters $\vec{\theta}_p$ are the phase shifters in the state preparation part and the U and $V(\vec{\theta})$ encoding circuits are kept identity. After the aligning, we prepared the optimal aligned state $|\phi(\vec{\theta}^{\text{opt}}_p)\rangle$ as input, encoded the target U, initialized the $V(\vec{\theta})$, and conducted the consequent VEAPT optimization. Figure 3(c) gives the error mitigation results on two-qubit cases, which further enhanced maximum F_{avg} to 95.56%. It is an illustrative example of quantum machine learning in solving several challenging tasks. Furthermore, we verified the influence of shot noises on our method in Fig. 3(d). By adjusting the

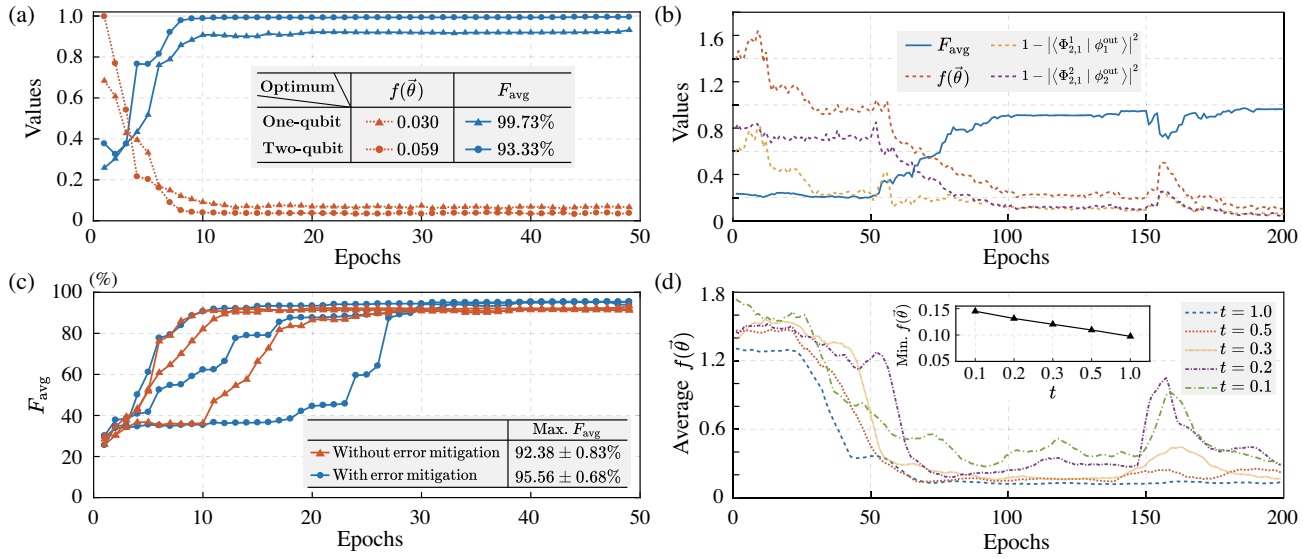

FIG. 3. Experimental demonstration of the VEAPT method. (a) VEAPT with full ancillary qubits on one-qubit (triangle) and two-qubit (circle) cases. The cost function $f(\vec{\theta})$ (red dotted lines) and the average gate fidelity F_{avg} (blue solid lines) gradually converge. Minimum $f(\vec{\theta})$ and maximum F_{avg} are listed in the table. (b) Two-qubit VEAPT with one ancillary qubit and two input states. The red dotted line is the overall cost function, while the yellow and purple ones show the corresponding infidelities between the output state and the two entangled states, respectively. (c) Error mitigation results on two-qubit cases, where the blue circle and red triangle lines are different trials with and without error mitigation, respectively. The final maximum F_{avg} is further enhanced to 95.56% after the error mitigation operation. (d) Two-qubit VEAPT with one ancillary qubit under different levels of shot noise. The vertical axis denotes the average cost function values among the past 10 epochs. In the inset graph, it is clear that longer integration time t with more photons achieves better performance. We used the BFGS algorithm in (a) and (c), while the SPSA algorithm is employed in (b) and (d).

photon integration time t, we can obtain different shot noise levels. When the integration time t is small, the corresponding photon counting rate is low and the shot noise level is relatively high. It can be seen that the optimization procedure may be longer with shorter t. More details are provided in the Supplemental Material [32].

Conclusion.—Quantum process tomography is an increasingly important certification and benchmarking tool for quantum computing devices with the full information gain. In this Letter, we put forward an efficient, flexible, and error-mitigated VEAPT method with arbitrary ancillary qubits, which is promising for practical usage in the NISQ era. Numerically, we simulated up to eight-qubit quantum processes showing that VEAPT with m ancillary qubits ($0 \le m \le n$) alleviates the exponential costs on state preparation (from 4^n to 2^{n-m}), measurement settings (at least 1 order of magnitude fewer than standard QPT), and data postprocessing (efficient and robust parameter optimization). Experimentally, we first demonstrated our method on a silicon photonic chip by reconstructing arbitrary one-qubit and two-qubit unitary quantum processes. Results show that those quantum processes can be rebuilt with average gate fidelity 99.73% and 93.33%, respectively. Moreover, we conducted error mitigation trials on two-qubit quantum processes presenting obvious enhancement to 95.56%. Our Letter provides an efficient, flexible, and error-mitigated approach to process tomography and can be used as a practical demonstration tool in larger-scale quantum computing devices in the NISQ era.

The authors acknowledge support from other members of the QUANTA (QUantum fANs from IT Area) group, including Yang Wang, Chao Wu, Pingyu Zhu, Yuzhen Zheng, Qilin Zheng, and Hao Cheng. The authors are grateful to Chu Guo and Siqi Wang for their useful discussions and technical support. The authors acknowledge the support from the National Natural Science Foundation of China under Grants No. 62061136011, No. 61632021, and No. 62105366.

*Corresponding author.
junjiewu@nudt.edu.cn
†These authors contributed equally to this work.

[1] F. Arute, K. Arya, R. Babbush, D. Bacon, J. C. Bardin, R. Barends, R. Biswas, S. Boixo, F. G. Brandao, D. A. Buell *et al.*, Quantum supremacy using a programmable superconducting processor, Nature (London) **574**, 505 (2019).

[2] P. Jurcevic, A. Javadi-Abhari, L. S. Bishop, I. Lauer, D. F. Bogorin, M. Brink, L. Capelluto, O. Günlük, T. Itoko, N. Kanazawa *et al.*, Demonstration of quantum volume 64 on a superconducting quantum computing system, Quantum Sci. Technol. **6**, 025020 (2021).

[3] Y. Wu, W.-S. Bao, S. Cao, F. Chen, M.-C. Chen, X. Chen, T.-H. Chung, H. Deng, Y. Du, D. Fan *et al.*, Strong Quantum Computational Advantage Using a Superconducting Quantum Processor, Phys. Rev. Lett. **127**, 180501 (2021).

[4] A. W. Cross, L. S. Bishop, S. Sheldon, P. D. Nation, and J. M. Gambetta, Validating quantum computers using randomized model circuits, Phys. Rev. A **100**, 032328 (2019).

[5] J. Preskill, Quantum computing in the NISQ era and beyond, Quantum **2**, 79 (2018).

[6] M. Brooks, Beyond quantum supremacy: The hunt for useful quantum computers, Nature (London) **574**, 19 (2019).

[7] N. Moll, P. Barkoutsos, L. S. Bishop, J. M. Chow, A. Cross, D. J. Egger, S. Filipp, A. Fuhrer, J. M. Gambetta, M. Ganzhorn *et al.*, Quantum optimization using variational algorithms on near-term quantum devices, Quantum Sci. Technol. **3**, 030503 (2018).

[8] S. T. Flammia and Y.-K. Liu, Direct Fidelity Estimation from Few Pauli Measurements, Phys. Rev. Lett. **106**, 230501 (2011).

[9] E. Knill, D. Leibfried, R. Reichle, J. Britton, R. B. Blakestad, J. D. Jost, C. Langer, R. Ozeri, S. Seidelin, and D. J. Wineland, Randomized benchmarking of quantum gates, Phys. Rev. A **77**, 012307 (2008).

[10] E. Magesan, J. M. Gambetta, and J. Emerson, Scalable and Robust Randomized Benchmarking of Quantum Processes, Phys. Rev. Lett. **106**, 180504 (2011).

[11] I. L. Chuang and M. A. Nielsen, Prescription for experimental determination of the dynamics of a quantum black box, J. Mod. Opt. **44**, 2455 (1997).

[12] J. F. Poyatos, J. I. Cirac, and P. Zoller, Complete Characterization of a Quantum Process: The Two-Bit Quantum Gate, Phys. Rev. Lett. **78**, 390 (1997).

[13] M. Mohseni, A. T. Rezakhani, and D. A. Lidar, Quantum-process tomography: Resource analysis of different strategies, Phys. Rev. A **77**, 032322 (2008).

[14] K. Banaszek, G. M. D'Ariano, M. G. A. Paris, and M. F. Sacchi, Maximum-likelihood estimation of the density matrix, Phys. Rev. A **61**, 010304(R) (1999).

[15] C. Ferrie, Self-Guided Quantum Tomography, Phys. Rev. Lett. **113**, 190404 (2014).

[16] R. C. Bialczak, M. Ansmann, M. Hofheinz, E. Lucero, M. Neeley, A. D. O'Connell, D. Sank, H. Wang, J. Wenner, and M. Steffen, Quantum process tomography of a universal entangling gate implemented with Josephson phase qubits, Nat. Phys. **6**, 409 (2010).

[17] J. L. O'Brien, G. J. Pryde, A. Gilchrist, D. F. V. James, N. K. Langford, T. C. Ralph, and A. G. White, Quantum Process Tomography of a Controlled-NOT Gate, Phys. Rev. Lett. **93**, 080502 (2004).

[18] A. M. Childs, I. L. Chuang, and D. W. Leung, Realization of quantum process tomography in NMR, Phys. Rev. A **64**, 012314 (2001).

[19] A. Shabani, R. L. Kosut, M. Mohseni, H. Rabitz, M. A. Broome, M. P. Almeida, A. Fedrizzi, and A. G. White, Efficient Measurement of Quantum Dynamics via Compressive Sensing, Phys. Rev. Lett. **106**, 100401 (2011).

[20] M. Riebe, K. Kim, P. Schindler, T. Monz, P. O. Schmidt, T. K. Körber, W. Hänsel, H. Häffner, C. F. Roos, and R. Blatt, Process Tomography of Ion Trap Quantum Gates, Phys. Rev. Lett. **97**, 220407 (2006).

[21] L. Govia, G. Ribeill, D. Ristè, M. Ware, and H. Krovi, Bootstrapping quantum process tomography via a perturbative ansatz, Nat. Commun. **11**, 1084 (2020).

[22] Z. Hou, J.-F. Tang, C. Ferrie, G.-Y. Xiang, C.-F. Li, and G.-C. Guo, Experimental realization of self-guided quantum process tomography, Phys. Rev. A **101**, 022317 (2020).

[23] D. Gross, Y.-K. Liu, S. T. Flammia, S. Becker, and J. Eisert, Quantum State Tomography via Compressed Sensing, Phys. Rev. Lett. **105**, 150401 (2010).

[24] M. Cramer, M. B. Plenio, S. T. Flammia, R. Somma, D. Gross, S. D. Bartlett, O. Landon-Cardinal, D. Poulin, and Y.-K. Liu, Efficient quantum state tomography, Nat. Commun. **1**, 149 (2010).

[25] J. B. Altepeter, D. Branning, E. Jeffrey, T. C. Wei, P. G. Kwiat, R. T. Thew, J. L. O'Brien, M. A. Nielsen, and A. G. White, Ancilla-Assisted Quantum Process Tomography, Phys. Rev. Lett. **90**, 193601 (2003).

[26] G. M. D'Ariano and P. LoPresti, Quantum Tomography for Measuring Experimentally the Matrix Elements of an Arbitrary Quantum Operation, Phys. Rev. Lett. **86**, 4195 (2001).

[27] D. W. C. Leung, *Towards Robust Quantum Computation* (Stanford University, Stanford, 2000).

[28] M.-D. Choi, Completely positive linear maps on complex matrices, Linear Algebra Appl. **10**, 285 (1975).

[29] D. W. Leung, Choi's proof as a recipe for quantum process tomography, J. Math. Phys. (N.Y.) **44**, 528 (2003).

[30] G. M. D'Ariano and P. LoPresti, Imprinting Complete Information about a Quantum Channel on its Output State, Phys. Rev. Lett. **91**, 047902 (2003).

[31] F. De Martini, A. Mazzei, M. Ricci, and G. M. D'Ariano, Exploiting quantum parallelism of entanglement for a complete experimental quantum characterization of a single-qubit device, Phys. Rev. A **67**, 062307 (2003).

[32] See Supplemental Material at http://link.aps.org/supplemental/10.1103/PhysRevLett.129.133601 for the generality analysis of the VEAPT method, the details on the VEAPT experiment, the two algorithms for optimization, the details on the numerical simulation, and the design and realization on the error mitigation method.

[33] M. Cerezo, A. Arrasmith, R. Babbush, S. C. Benjamin, S. Endo, K. Fujii, J. R. McClean, K. Mitarai, X. Yuan, L. Cincio *et al.*, Variational quantum algorithms, Nat. Rev. Phys. **3**, 625 (2021).

[34] A. Peruzzo, J. McClean, P. Shadbolt, M.-H. Yung, X.-Q. Zhou, P. J. Love, A. Aspuru-Guzik, and J. L. O'brien, A variational eigenvalue solver on a photonic quantum processor, Nat. Commun. **5**, 4213 (2014).

[35] E. Farhi, J. Goldstone, and S. Gutmann, A quantum approximate optimization algorithm, arXiv:1411.4028.

[36] J. R. McClean, J. Romero, R. Babbush, and A. Aspuru-Guzik, The theory of variational hybrid quantum-classical algorithms, New J. Phys. **18**, 023023 (2016).

[37] S. Khatri, R. LaRose, A. Poremba, L. Cincio, A. T. Sornborger, and P. J. Coles, Quantum-assisted quantum compiling, Quantum **3**, 140 (2019).

[38] R. LaRose, A. Tikku, É. O'Neel-Judy, L. Cincio, and P. J. Coles, Variational quantum state diagonalization, npj Quantum Inf. **5**, 57 (2019).
[39] M. Cerezo, A. Poremba, L. Cincio, and P. J. Coles, Variational quantum fidelity estimation, Quantum **4**, 248 (2020).
[40] S. Endo, J. Sun, Y. Li, S. C. Benjamin, and X. Yuan, Variational Quantum Simulation of General Processes, Phys. Rev. Lett. **125**, 010501 (2020).
[41] X. Yuan, S. Endo, Q. Zhao, Y. Li, and S. C. Benjamin, Theory of variational quantum simulation, Quantum **3**, 191 (2019).
[42] S. Endo, S. C. Benjamin, and Y. Li, Practical Quantum Error Mitigation for Near-Future Applications, Phys. Rev. X **8**, 031027 (2018).
[43] S. Endo, Z. Cai, S. C. Benjamin, and X. Yuan, Hybrid quantum-classical algorithms and quantum error mitigation, J. Phys. Soc. Jpn. **90**, 032001 (2021).
[44] Y. Liu, D. Wang, S. Xue, A. Huang, X. Fu, X. Qiang, P. Xu, H.-L. Huang, M. Deng, C. Guo *et al.*, Variational quantum circuits for quantum state tomography, Phys. Rev. A **101**, 052316 (2020).
[45] S. Xue, Y. Liu, Y. Wang, P. Zhu, C. Guo, and J. Wu, Variational quantum process tomography of unitaries, Phys. Rev. A **105**, 032427 (2022).
[46] C. G. Broyden, The convergence of a class of double-rank minimization algorithms 1. general considerations, IMA J. Appl. Math. **6**, 76 (1970).
[47] R. Fletcher, A new approach to variable metric algorithms, Comput. J. **13**, 317 (1970).
[48] D. Goldfarb, A family of variable-metric methods derived by variational means, Math. Comput. **24**, 23 (1970).
[49] D. F. Shanno, Conditioning of quasi-Newton methods for function minimization, Math. Comput. **24**, 647 (1970).
[50] J. C. Spall *et al.*, Multivariate stochastic approximation using a simultaneous perturbation gradient approximation, IEEE Trans. Autom. Control **37**, 332 (1992).
[51] S. Boixo, S. V. Isakov, V. N. Smelyanskiy, R. Babbush, N. Ding, Z. Jiang, M. J. Bremner, J. M. Martinis, and H. Neven, Characterizing quantum supremacy in near-term devices, Nat. Phys. **14**, 595 (2018).
[52] C. Guo, Y. Liu, M. Xiong, S. Xue, X. Fu, A. Huang, X. Qiang, P. Xu, J. Liu, S. Zheng *et al.*, General-Purpose Quantum Circuit Simulator with Projected Entangled-Pair States and the Quantum Supremacy Frontier, Phys. Rev. Lett. **123**, 190501 (2019).
[53] M. Žnidarič, T. Prosen, and P. Prelovšek, Many-body localization in the Heisenberg *XXZ* magnet in a random field, Phys. Rev. B **77**, 064426 (2008).
[54] J. Wang, S. Paesani, Y. Ding, R. Santagati, P. Skrzypczyk, A. Salavrakos, J. Tura, R. Augusiak, L. Mančinska, D. Bacco *et al.*, Multidimensional quantum entanglement with large-scale integrated optics, Science **360**, 285 (2018).
[55] X. Qiang, X. Zhou, J. Wang, C. M. Wilkes, T. Loke, S. O'Gara, L. Kling, G. D. Marshall, R. Santagati, T. C. Ralph *et al.*, Large-scale silicon quantum photonics implementing arbitrary two-qubit processing, Nat. Photonics **12**, 534 (2018).
[56] X. Qiang, Y. Wang, S. Xue, R. Ge, L. Chen, Y. Liu, A. Huang, X. Fu, P. Xu, T. Yi *et al.*, Implementing graph-theoretic quantum algorithms on a silicon photonic quantum walk processor, Sci. Adv. **7**, eabb8375 (2021).
[57] M. A. Nielsen, A simple formula for the average gate fidelity of a quantum dynamical operation, Phys. Lett. A **303**, 249 (2002).